https://doi.org/10.5194/egusphere-2023-940
Preprint. Discussion started: 12 May 2023

Increase in precipitation scavenging contributes to long-term reductions of black carbon in the Arctic.

Dominic Heslin-Rees[1,2], Peter Tunved[1,2], Johan Ström[1,2], Roxana Cremer[1,2], Paul Zieger[1,2], Ilona Riipinen[1,2], Annica Ekman[2,3], Konstantinos Eleftheriadis[4], and Radovan Krejci[1,2]

[1]Department of Environmental Science, Stockholm University, Stockholm, Sweden
[2]Bolin Centre for Climate Research, Stockholm University, Stockholm, Sweden
[3]Department of Meteorology (MISU), Stockholm University, Stockholm, Sweden
[4]Institute of Nuclear Technology—Radiation Protection, N.C.S.R. "Demokritos", Athens, Greece

Correspondence: Dominic.Heslin-Rees@aces.su.se

Abstract.

Black carbon (BC), the most efficient atmospheric aerosol for absorbing light in the visible spectrum, exerts a warming effect on a region undergoing unprecedented climatic changes. Here, BC is studied indirectly using filter-based methods to ascertain aerosol light absorption parameters. We investigated long-term changes using a harmonised 21-year data set of light absorption measurements, in conjunction with air mass source analysis. The measurements were performed at Zeppelin Observatory (ZEP), Svalbard, from 2002 to 2022. We report a statistically significant (s.s.) decreasing long-term trend for the light absorption coefficient, measured at the site for the entirety of the data set. However, the last 7 years, 2016-2022, showed a slightly increasing s.s. trend in the haze season. In addition, we observed an increasing trend in the single scattering albedo from 2002 to 2022. Five distinct source regions were identified; the trends involving air masses from the five regions showed decreasing absorption coefficients, except for the air masses influenced by emissions from Eurasia. We show that the changes in the occurrences of each transport pathway cannot explain the reductions in the absorption coefficient observed at the Zeppelin station; an increase in contributions of air masses from more marine regions, with lower absorption coefficients, is compensated by the influence from high-emission regions. Along with aerosol optical properties, we also show an increasing trend in accumulated surface precipitation experienced by air masses en route to the Zeppelin Observatory. We argue that rainfall, as a sink of aerosol, plays a role in the long-term trends in the absorption coefficient, explaining approximately a quarter of the overall trend. A decreasing trend in the scavenging ratio further suggests an increase in the aerosol removal processes. We note that there is an increasing potential influence from active forest fires, particularly in the last few summers (i.e. 2015 - 2022). Active fires have been shown to have a significant impact on the mean seasonal absorption coefficient especially during northern hemispheric summer. However, no noticeable alteration in annual long-term trends can be observed.

https://doi.org/10.5194/egusphere-2023-940
Preprint. Discussion started: 12 May 2023

1 Introduction

The Arctic region has undergone increased rates of warming compared to the global average (Rantanen et al., 2022), a phenomenon known as Arctic Amplification (AA). Although the main driver of AA is the increased concentrations of greenhouse gases and related feedbacks in the climate system, suspended particles in the atmosphere, i.e. aerosol, could still be an important factor in explaining AA (Shindell and Faluvegi, 2009; Hansen and Nazarenko, 2004). Despite the relatively short lifetime of aerosol particles compared to other climate forcers, they are still able to exert a major influence on climate. Light-absorbing aerosol particles, such as black carbon (BC), can induce radiative warming whilst being suspended in the atmosphere. Furthermore, the deposition of BC on snow and ice increases the impact light-absorbing aerosols can have in all semi-persistent snow areas, such as polar environments, by reducing the albedo and enhancing the melting of snow and ice. Given the short lifetime of BC and its potential impact, any immediate reductions can lead to reduced radiative forcings within a short period, making BC mitigation a highly pertinent issue concerning the Arctic climate (Sand et al., 2016; AMAP, 2015).

Light-absorbing aerosols cover a broad range of aerosol types, with the major component being BC. BC can be of both natural and anthropogenic origin, with BC being a product of incomplete combustion from biomass and fossil fuels (sources include, for example, diesel engines, agricultural burning, wildfires, and residential heating). As a result, BC exists only as a primary aerosol. BC can be measured by utilising a specific property, the ability to attenuate light, at a given wavelength (λ). The light absorption coefficient (σ_{ap}) describes the amount of attenuation, per given length unit. The Arctic surface temperature response to the direct effects of light-absorbing particles is considered significant (AMAP, 2015). In addition, aged light-absorbing aerosols, of sufficient hygroscopicity and size, can also act as cloud condensation nuclei (CCN) (Dalirian et al., 2018), and thus influence cloud properties. For most Arctic sites, including Svalbard, Europe and Asia are considered the main contributors to BC loadings (Winiger et al., 2019; Backman et al., 2014; Shaw, 1982). It is well known that agricultural and boreal forest fire events can dominate aerosol loading for periods at a time (Stohl et al., 2007). In summer the elemental carbon (EC; a mass-based BC analogue) typically originates from biomass burning (BB) at lower latitudes (Winiger et al., 2019). In winter and spring, the proportion of Zeppelin EC from BB decreases (Winiger et al., 2015). Russian gas flaring is considered another potential major source of BC, however, direct measurement of its respective contribution is lacking (Winiger et al., 2019).

Like other aerosol particles, BC can be transported over large distances, ending up in pristine environments such as the Arctic. Aerosols in the Arctic exhibit a pronounced seasonality (Tunved et al., 2013), in which mass concentrations are high during late winter and early spring, a period known as the Arctic Haze, and low during summer (Shaw, 1995; Freud et al., 2017). The Arctic Haze phenomenon is the result of aerosol particles from areas of high emission being transported to the Arctic under favourable transport conditions, with low removal, low turbulent mixing and fewer frontal passages (Quinn et al., 2007; Garrett et al., 2011). The seasonality of the phenomenon is governed mainly by removal processes (Garrett et al., 2011). The Arctic Haze demonstrates the potential anthropogenic influence regions further south can have on the Arctic.

To understand whether the transformations, most notably the increase in sea surface temperatures, taking place in the Arctic can be linked to changes in aerosol concentrations, long-term monitoring of key meteorological and aerosol parameters is

https://doi.org/10.5194/egusphere-2023-940
Preprint. Discussion started: 12 May 2023

required. The Arctic poses numerous challenges when it comes to carrying out measurements. The techniques required need to be particularly sensitive, due to the low aerosol loadings. (i.e. approximately in the tens of ng/m^{-3}) (Sinha et al., 2017a; **?**). The anthropogenic influence on the Arctic from regions further south has been established for decades (Shaw, 1982; Stohl et al., 2007). Furthermore, the continuous monitoring of atmospheric pollutants in the Arctic has given rise to some important long-term time series showing changes in atmospheric composition taking place. For certain sites, it is now possible to analyse the changes observed in aerosol properties on a climatic time scale, making sites such as the Zeppelin Observatory of great importance when aiming to perform a statistically robust analysis (Platt et al., 2022). The advent of cleaner combustion techniques has led to significant declines in sulphate aerosol loadings (Acosta Navarro et al., 2016); however, during the same period BC global emissions continued to increase due to increased emissions mainly from Asia (Klimont et al., 2017; Schmale et al., 2022). The use of in situ surface measurements allows for the monitoring of air pollutants without having to rely on emission inventories, which are associated with large uncertainties (Winiger et al., 2019; Bond et al., 2013). Numerous studies have reported on the decline in BC concentrations measured from the Arctic (Sharma et al., 2013; Collaud Coen et al., 2020; Bodhaine and Dutton, 1993; Schmale et al., 2022). The time series presented here is over two decades long as a result of the successful harmonisation of the measurement series. Many have hypothesised that the decrease in BC concentrations in the Arctic is the result of reductions in pollution from Europe and the former Soviet Union (FSU), in part due to stricter pollution controls (Sharma et al., 2013). However, there is a lack of studies which substantiate the factors for the observed trends in BC concentrations in the Arctic. In particular, the role that aerosol sinks could play when it comes to trends has received little attention (Garrett et al., 2011). This lack of investigation into the role scavenging can have on aerosol concentrations could be one of the reasons why models overestimate observed BC (Sharma et al., 2013), and also why there is a pronounced difference between trends in atmospheric and BC ice core measurements (Ruppel et al., 2017, 2014).

In this study, in situ measurements of atmospheric light-absorbing aerosol particles are used to explore how concentrations have changed over two decades from 2002 to 2022. In the knowledge that concentrations of BC in the Arctic depend on a range of factors including emissions, meteorological conditions and atmospheric dynamics promoting certain transportation pathways, and the effectiveness of various removal processes in the atmosphere, multiple factors within the context of sources, sinks, and transport will be analysed. To understand how aerosols can be influenced by changes in wet scavenging, this study will examine the long-term trends in the surface accumulated precipitation en route towards the Zeppelin Observatory. In this study, our objective is to explore the links between Arctic BC concentrations and wet removal processes over the course of a climatically relevant time period. The main research questions that this work aims to tackle are as follows: (i) What are the long-term trends in the absorption coefficient (σ_{ap}) and the single scattering albedo (SSA) at the Zeppelin Observatory? (ii) What are the key factors controlling these trends (e.g. changes in scavenging, transport pathways and/or sources)? (iii) Can precipitation explain clean-day events (i.e. when σ_{ap} is low)? (iv) Are the calculated long-term trends in σ_{ap} influenced by extreme events (e.g. boreal forest fires for dirty and high precipitation rates for clean events)?, (vi) Which source regions contribute most to observed BC concentration at Zeppelin Observatory?

https://doi.org/10.5194/egusphere-2023-940
Preprint. Discussion started: 12 May 2023

2 Materials and Methods

2.1 Measurement site

Measurements were carried out at the Zeppelin Observatory (78.90°N, 11.88°E), hereafter referred to as ZEP. ZEP is located close to the research village Ny-Ålesund, on the western edge of Svalbard within the Kongsfjorden. ZEP is situated atop a mountain at an altitude of 474 m a.s.l., its distance from the nearby research village, wind conditions and the stratification of air masses mean that the measurements are not so affected by local pollution. The remoteness of the observatory, and the pristine environment that it is located in, means that it is representative of regional background Arctic conditions. ZEP is part of several regional and global monitoring networks including the Global Atmosphere Watch (WMO/GAW), Integrating Carbon Observation System (ICOS), The Aerosol, Clouds and Trace Gases Research Infrastructure (ACTRIS) and European Monitoring and Evaluation Programme (EMEP). For further details on the observatory and past research see Platt et al. (2022).

2.2 Description of Instrumentation:

The absorption coefficient measurements are from a range of different instrumentation (see Fig. S1 in the supplementary information, SI). Below follows a more detailed description of the instruments used for deriving the σ_{ap}, as well as a short introduction to the nephelometers used for measuring the particle light scattering coefficient (hereafter σ_{sp}). All instrumentation measuring aerosol particles, mentioned in this study, were connected to the same whole-air inlet which follows guidelines set out by WMO/GAW for aerosol sampling (Zhongming et al., 2016), similar to the inlet described by Weingartner et al. (1999). The station itself and the whole-air inlet are both slightly heated, meaning no additional drying of the aerosol is required as the relative humidity of sample air inside the station is kept below 30-40%. In addition, the absorption coefficient from the homogenised time series was compared with data from an Aethalometer (Eleftheriadis et al., 2009; Stone et al., 2014; Sharma et al., 2013), which is a filter-based multi-wavelength optical method.

2.2.1 Particulate Soot Absorption Photometer

The custom-built Particle Soot Absorption Photometer (PSAP-ITM) with a manual filter loader (hereafter referred to as "manual PSAP") was developed by the Department of Applied Environmental Science (ITM) at Stockholm University. The manual PSAP operated from March 2002 to March 2013 (see Fig S1), whereby it was effectively replaced by another PSAP-ITM, this time with an automatic filter-loader (hereafter, "automatic PSAP"). The automatic PSAP, using the same type of filter and operating principle, operated from November 2012 to October 2016. The manual and automatic PSAPs operated at a wavelength of approximately 525 nm. For further details on the specifics of the PSAP-ITM see Krecl et al. (2007, 2010).

The PSAP works by measuring the change in the light transmission through a collection filter induced by laden aerosol particles. The attenuation of light is measured relative to a reference filter. The aerosol particles were collected on Tissuglass E70-2075W filters (Pall Corporation) with a diameter of 90 mm. Typically, the sample flow was around $1\,\mathrm{l\,min^{-1}}$. The sample

https://doi.org/10.5194/egusphere-2023-940
Preprint. Discussion started: 12 May 2023

spot for the custom-made PSAP is much smaller than the commercial instrument ($\approx$ 3.19 mm in diameter), which allows for lower detection limits for a given sample rate.

For the PSAP, there are two main issues associated with measuring the σ_{ap}, namely the artefacts due to multiple scattering from the filter itself and light scattering particles, and the influence of filter loading (see Müller et al. (2011a) for further details). Despite the artefacts related to filter-based aerosol absorption measurements, this method exhibits high sensitivity and is simple, robust, and widely used.

2.2.2 Multi Angle Absorption Photometer

Multi-Angle Absorption Photometer (MAAP, Thermo Fisher Scientific Inc., Germany, Model 5012) measured from 2014 to present. The MAAP utilises the same filter-based principle as the PSAP. However, the MAAP measures the incident radiation penetrating through the filter and simultaneously the radiation scattered back from the filter at two detection angles θ = 130° and 165° (Petzold and Schönlinner, 2004). The MAAP derives an absorption coefficient using radiative transfer calculations, developed by Hänel (1987), with modifications suitable for the evaluation of MAAP data developed by Kopp et al. (1999). The radiative transfer model takes into account multiple scattering effects between the particle-loaded filter layer and the particle-free filter matrix and also the scattering within the aerosol layer. MAAP has been widely used as a reference method (Asmi et al., 2021; Müller et al., 2011a). The operational wavelength of the MAAP is assumed to be 637 nm (Petzold et al., 2005; Müller et al., 2011a).

2.2.3 Nephelometers

Two integrating nephelometers (Ecotech Pty Ltd., Australia, model Aurora 3000 and TSI Inc., USA, model 3563) were used at ZEP throughout this study. The TSI nephelometer has been used since May 1999. The Ecotech nephelometer was installed in April 2018 and has been operated continuously since (see Platt et al. (2022) for further details). Both nephelometers utilise the same principle to perform continuous measurements of the light scattering of particles; the TSI and Ecotech perform measurements at three wavelengths (λ=450, 550, 700 nm and λ=450, 525, 635 nm respectively). Nephelometers are regularly calibrated using CO_2 and particle-free air. The contribution of light scattering by air molecules is automatically corrected by regular zero measurements of particle-free air, about every hour. Corrections to the measurements are necessary to account for the light source and angular non-idealities. The correction methods described in Anderson and Ogren (1998) and Müller et al. (2011b) were used to correct both the TSI and Ecotech nephelometer data respectively and applied to the hourly arithmetic means.

2.3 Back trajectory analysis

The history of air masses arriving at ZEP was analysed using the Hybrid Single-Particle Lagrangian Integrated Trajectory model (HYSPLIT V5.2.1) (Draxler and Hess, 1998; Stein et al., 2015). An ensemble of 27 back trajectories was initialised for every hour. The ensemble was generated by creating 3 planes, consisting of 9 starting points, whereby the meteorological field

https://doi.org/10.5194/egusphere-2023-940
Preprint. Discussion started: 12 May 2023

is shifted as opposed to the initial starting point. The air parcels in the model arrive at an altitude of 250 m above the ground to avoid any issues related to the displacement of the ensemble members. The back trajectories were run for 10 days back in time, a compromise between capturing potential source regions and the increased uncertainty in back trajectories with time. It should be noted that there was a change in the meteorological database used for the HYSPLIT back trajectories (at the end of 2005, the beginning of 2006). The choice of input meteorological fields is considered the most important factor contributing to uncertainties (Dadashazar et al., 2021; Gebhart et al., 2005). The meteorological fields were obtained from the National Oceanic and Atmospheric Administration (NOAA); the period 2002–2005 uses the FNL (Final) Operational Global Analysis archive data from The National Weather Service's National Centers for Environmental Prediction (NCEP), and 2006–2021 uses the Global Data Assimilation System (GDAS) 1° x 1° archive data. (http://ready.arl.noaa.gov/archives.php, last access: 02 12 2022). GDAS has been used in a previous analysis of ZEP (e.g. Tunved et al. (2013)). For the analysis, here, a 1°x1 ° rotated grid was initialised such that ZEP acted as the new north pole. To obtain continuous coverage of surface precipitation along the air mass transport pathway, the back trajectories were temporally and spatially collocated with fifth-generation ECMWF reanalysis (ERA5) hourly surface level data (Hersbach et al., 2018), such that each endpoint of the back trajectories was matched with the total surface precipitation variable from ERA5, for their respective geographical and temporal position. The accumulated surface precipitation was calculated by integrating along the back trajectory; hereafter, this parameter will be referred to as the accumulated trajectory precipitation (ATP). Given that the ERA5 precipitation data corresponds to surface data, then the calculated ATP value represents the maximum potential amount of precipitation experienced by the air mass parcel throughout its journey to the station as if the air parcel had travelled near the surface for the entire time period.

2.4 Data treatment

The data cover the period from 2002 to 2022; with each instrument operational at different periods of time (see Fig. S1). Instead of imposing a mass absorption cross-section coefficient (MAC) value and estimating the equivalent black carbon (eBC), only the optical-derived absorption coefficient is utilised.

For this study, the operational wavelength of the MAAP, λ=637 nm is used for all-optical properties that depend on the choice of λ, unless otherwise stated; σ_{ap} measurements from instruments with different operational wavelengths were adjusted to λ=637 nm (see eq. 2). Moreover, all data sets were corrected for standard temperature and pressure (STP, temperature 273.15 K and pressure 1 atm). Aerosol loadings are exceptionally low at ZEP most of the year (Platt et al., 2022), and thus the instruments are measuring close to their limit of detection (Asmi et al., 2021). In general, it is necessary for instruments to be well-calibrated due to the high noise-to-signal ratio. Moreover, aerosols at ZEP exhibit a single scattering albedo close to unity (Schmeisser et al., 2018), which can pose additional challenges as the correction schemes utilised are sensitive to high SSA (Bond et al., 1999). For the automatic and manual PSAPs this is not so much of a problem except in summer. Measurements of absorption and scattering are made sub-hourly. For all data sets, hourly arithmetic means are calculated and used to improve the signal-to-noise ratio. All data sets are temporally collocated. For simplicity, after re-sampling to hourly arithmetic means, all positive values were deemed valid (i.e. measurements $>0\,\mathrm{Mm}^{-1}$) despite the differences in sensitivity of the MAAP and PSAPs. It is

https://doi.org/10.5194/egusphere-2023-940
Preprint. Discussion started: 12 May 2023

understood that measurements below the detection limits exhibit large errors. Asmi et al. (2021) showed for an Arctic site with 1 hr temporal average, detection limits of 0.012 and 0.002 Mm^{-1} for the MAAP and PSAP respectively could be used.

2.4.1 Harmonisation

The analysis includes the harmonisation of over twenty years worth of absorption coefficient measurements from various instrument measurements. It should be noted that this work is not an intercomparison of instrumentation under controlled settings; for such work see for example Asmi et al. (2021); Ogren et al. (2017); Sinha et al. (2017b). Instead, the aim here is to describe the evolution of the measurements over time, given all the changes to instrumentation at ZEP from 2002 to 2022 e.g. calibrations and maintenance.

The temporal evolution for the relation between the measurements recorded by the MAAP and automatic PSAP is fairly constant (see Fig. S2), as such applying a single correction factor (i.e. 0.61) to the measurements from the automatic PSAP seemed justified (see Fig. S3). As a result of the comparison between the measurements of the manual PSAP and the automatic PSAP with the aforementioned CF applied, a constant value of 1.30 for this CF was applied to the manual PSAP measurements. Moreover, the period in which the automatic PSAP and manual PSAP overlapped is limited to winter and early spring, which could have implications for this CF. Comparisons of how the measurements from the various instruments have changed are given in section 2 in the supplement. Additionally, a comparison between each set of instrument measurements is compared with the long-term data set of absorption coefficient measurements from an Aethalometer (adjusted to 637 nm; see also Stathopoulos et al. (2021) and Fig. S4).

The harmonisation allows for the generation of a time series that acts as one of the longest sets of measurements for σ_{ap} in the Arctic (with Alert, Kevo and Barrow having longer time series, see Schmale et al., 2022).

2.4.2 Trend analysis

Aerosol optical properties are typically not normally distributed, and as a result, many statistical methods are not suitable, for analysis of scattering and absorption data (Collaud Coen et al., 2020). Observations of σ_{ap} and σ_{sp} are better represented by log-normal distributions (Collaud Coen et al., 2020). Medians are utilised for the trend analysis of σ_{ap} and σ_{sp} because of the non-Gauissan nature of the data distribution, and the fact that the use of medians is more robust against outliers. For all other variables though, including the accumulated back trajectory precipitation (ATP), number of active numbers and emissions of black carbon, the arithmetic mean is utilised to perform the trend analysis.

In accordance with previous trend analysis studies (Collaud Coen et al., 2020, 2013; Asmi et al., 2013), the Mann-Kendall test, Seasonal Mann-Kendall test (hereafter "MK test" and "Seasonal MK test") and Theil-Sen estimator (TS) are utilised to estimate the statistical significance (s.s.) and magnitude of various long-term trends respectively. The MK is performed on a two-tailed significance test of 95% to ascertain the s.s. The MK test and TS are non-parametric and are thus suitable for use with σ_{ap} and σ_{sp}. A combination of daily, monthly and seasonal arithmetic means & medians are used throughout the study, to provide a range of resolutions that incorporate a range of data amount and degrees of autocorrelation. For daily averages, when the data is more likely to be plagued by autocorrelation, the data is "pre-whitened" using the three prewhitening method (3PW)

https://doi.org/10.5194/egusphere-2023-940
Preprint. Discussion started: 12 May 2023

(Collaud Coen et al., 2020). In keeping with similar studies (e.g. Collaud Coen et al. (2020)), daily averages were computed with the requirement that at least 25% of the day consists of valid data (i.e. ∼6 hrs). For more details about TS see Sen (1968); for the MK test see Hirsch et al. (1982); Gilbert (1987).

The Arctic aerosol seasons, used throughout this study, are defined as follows:

- Arctic Haze (AHZ), February - May: Enhanced concentration of accumulation mode aerosol. Transport is characterised by low amounts of precipitation, on average 2-3 mm of rain experienced by air masses during the 10 days prior to arrival (Tunved et al., 2013).
- Summer (SUM), June - September: Decreased concentrations of accumulation mode aerosol particles and enhanced concentrations of Aitken and nucleation mode particles characterise summer months. SUM experiences the highest amounts of precipitation, on average 7-8 mm of rain prior to arrival (Tunved et al., 2013).
- Slow-build up (SBU), October - January: SBU is characterised as a transition period, in which the concentration of accumulation mode particles begins to increase towards the end of the season, "building" back up to the concentrations observed AHZ seasons. The SBU season experiences little sunlight with the polar night starting in November and ending in late January.

2.4.3 Air mass backward trajectory analysis

Back trajectories were classified into different air transportation pathways using a *k*-means clustering method. The *sklearn.cluster* Python package is used *scikit-learn*, v.1.2.1 (Pedregosa et al., 2011). The *k*-means clustering algorithm was performed on coordinates transformed from geographic (i.e. latitude, longitude and altitude) to their equivalent Cartesian coordinates (i.e. x,y,z). The *k*-means clustering was performed on back trajectory ensembles (i.e. 27 back trajectories per each hour). Furthermore, the data were temporally collocated with the absorption data set such that only timestamps in which both data sets had valid data were used. In order to assign a cluster to each measurement a criterion was imposed such that more than 50% of the 27 ensemble had to have been assigned the same cluster. By specifying this criterion 90% of the data remained and ensembles with a mixed back trajectory/air mass origin are removed (see Fig. S5). By identifying the transportation pathways, enables trends of certain regions to be explored in more detail, and for certain rain-aerosol relationships to be more closely analysed. Furthermore, the back trajectories were utilised to develop concentration weight trajectory (CWT) in line with Hsu et al. (2003). This enabled a spatial overview of the various source regions. However, there is still the possibility that, given the spatial limitations, various source regions are beyond the reach of 10-day back trajectories.

2.4.4 Scavenging ratio

To study the effects of wet removal processes on aerosol particles during long-range transport, the method by Garrett et al. (2011) is used. The method essentially normalises the in situ aerosol measurements by the concentration of carbon monoxide (CO), a compound which is reasonably inert and typically co-emitted with pollution events (Dadashazar et al., 2021). Moreover,

https://doi.org/10.5194/egusphere-2023-940
Preprint. Discussion started: 12 May 2023

CO is relatively insensitive to wet scavenging processes and has an average atmospheric lifespan considerably longer than aerosol particles. Using CO to quantify the wet removal during transport has been done by plenty of studies in the past (e.g. Oshima et al., 2012). For this study, it was not possible to use hourly averages, as recommended in the study by Garrett et al. (2011), instead daily CO means were utilised.

2.5 Forest fires identification

The Global Emission Fire Database (GFED) combines information from different satellite and in situ data (Van Der Werf et al., 2017). The fourth version of the GFED is used in partnership with the HYSPLIT back trajectory data to estimate the fires and subsequent BC emissions which could potentially be transported to ZEP. In addition to GFED, the number of active forest fires recorded by MODIS was used to provide a fire count for each back trajectory. For the GFED, it was combined with HYSPLIT by summing up the emissions of BC within each traversed grid cell. The number of active fires was combined with HYSPLIT by summing up the number of active fires within each 1°x1° grid and then counting the number of total active fires for each grid a back trajectory traversed over whilst in the mixing layer, as defined by the HYSPLIT model (see example Fig. S6). Li et al. (2020) found large uncertainties predicting the effects of BB effects with trajectory models, however, noted that the use of ensemble means displayed the best performance.

https://doi.org/10.5194/egusphere-2023-940
Preprint. Discussion started: 12 May 2023

3 Results

Here, the first section (section 3.1) describes the long-term trends in the absorption coefficient and single scattering albedo. Sections 3.2 - 3.5 are devoted to understanding the trends with respect to transport, sinks and sources.

3.1 Trends in optical properties

3.1.1 Long-term trend in absorption coefficient and single scattering albedo

Overall, the last 21 years of observations (2002 - 2022) have displayed a statistically significant (s.s.) negative trend in σ_{ap}. The long-term trend, based on seasonal medians, is approximately -0.004 (-0.0063 to -0.0016) $Mm^{-1}yr^{-1}$ (see Fig. 1). In relative terms (i.e. the ratio of the trend over the average), the negative trend in σ_{ap} corresponds to -4.3 % yr^{-1}. The trend based on daily medians corresponds to a s.s. -0.001 $Mm^{-1}yr^{-1}$, after correcting for autocorrelation. Furthermore, all seasons experience decreasing trends, with the Arctic Haze season displaying the largest decrease in absolute terms (s.s. decreasing trends based on 3PW daily medians are -0.002, -0.001, -0.001 for the seasons AHZ, SBU, and SUM respectively). The full-time series is probably not best explained using a single trend, but instead, the data exhibit two regimes, one with a decreasing trend and another with an increasing trend, starting around 2016 (see Fig. S7). For the period after 2016, only the AHZ displays a positive s.s. (p=0.003) trend of 0.01 $Mm^{-1}yr^{-1}$ based on daily medians. Overall, the temporal aggregation is not homogeneous to deem the trend after 2016 to be s.s. for all seasons.

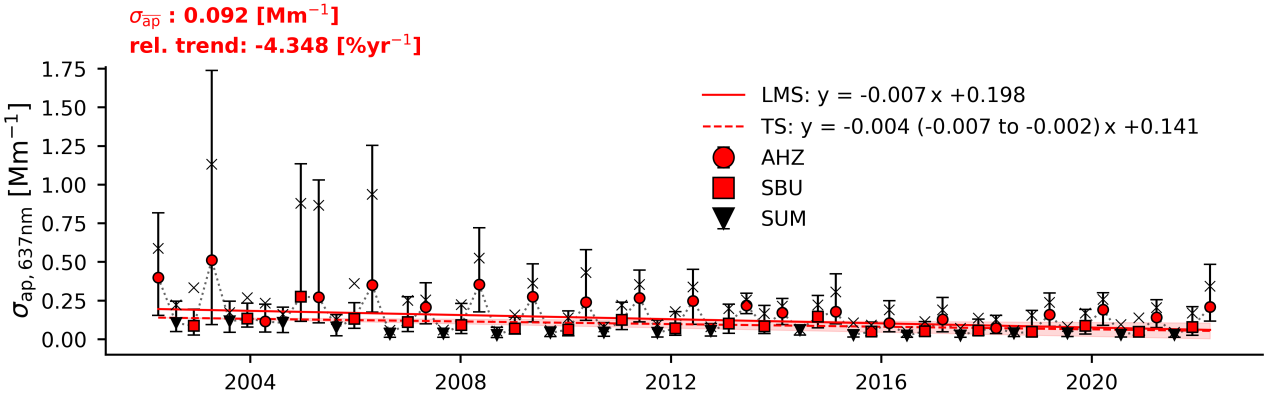

Figure 1. Harmonised time series for the absorption coefficient (σ_{ap}) measured at Zeppelin observatory: seasonal medians are displayed as shapes, the Arctic Haze (AHZ) denoted by a red circle, the slow-build up (SBU) by a red square and summer (SUM) by a black triangle. The error bars represent the 25 th and 75 th seasonal percentiles. The Theil-Sen Slope (TS) trend line is displayed as a dashed red line with a red-shaded region corresponding to 95% significance. The least-mean square (LMS) is presented as a solid red line. The trend lines are both calculated using the seasonal medians (various shapes), as opposed to seasonal means (cross). The overall median for the data set is displayed in the top left, along with the relative trend which is the TS slope divided by the median.

https://doi.org/10.5194/egusphere-2023-940
Preprint. Discussion started: 12 May 2023

The single scattering albedo has experienced an increase in the last 21 years from 0.9 to close to 1 (see Fig. S8). During this period of time, SSA has increased because of a long-term increase in σ_{sp} in conjunction with a decrease in σ_{ap}.

3.2 Sources, sinks and transport

3.2.1 Concentration weighted trajectories

Concentration-weighted trajectory (CWT) mappings are used to identify potential source areas; σ_{ap} measured at ZEP is weighted based on the time back trajectories spend traversing each grid cell within the mixing layer. CWT mappings possess information on sources, sinks and transport. Grid cells with higher CWT values suggest that these areas contribute more to the absorption coefficient measured at ZEP. It is apparent that regions around north-central Eurasia contribute the most to the measured σ_{ap}, however, there is an interannual variability (see Fig. S9). We have performed a spatial and temporal trend analysis on the CWT mappings (see Fig. 2). Essentially, the trend is calculated for each and every grid cell on an annual resolution (a seasonal trend was also performed with little difference, and for sake of simplicity the annual trend is displayed).

Figure 2 signifies that the largest declines in the CWT value occurred in the FSU region (i.e. central Eurasia). Furthermore, we can ascertain that the long-term trends in the CWT value are mainly negative, with a slight increase in the contribution originating either in south-eastern Europe or beyond (i.e. regions neighbouring the Caspian and Black seas). The results here resemble the trends in the emission inventories (see Fig. S10). Due to limitations with the extent to which back trajectories can reliably go backwards the CWT trend mapping does not convey the entire northern hemisphere.

https://doi.org/10.5194/egusphere-2023-940
Preprint. Discussion started: 12 May 2023

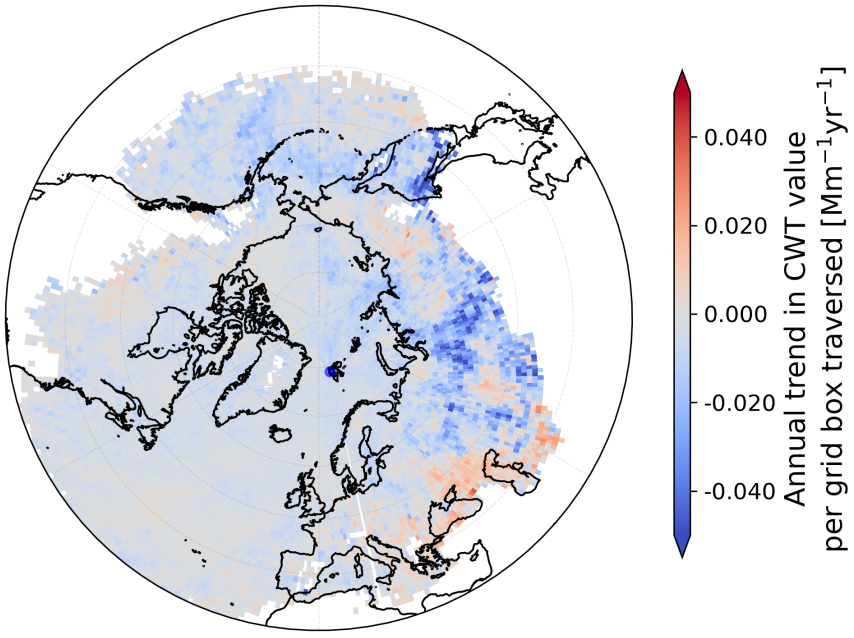

Figure 2. Long-term trend in the annual CWT values for σ_{ap}, for years 2002 - 2022. A threshold is 15 data points for each 1°x1° grid cell is applied to the mapping (out of a possible 21).

3.3 Transport

3.3.1 Trajectory source analysis

The cluster analysis, whereby a total of 5 different clusters each signifying a potential transport pathway, are shown in Fig. 3. Typically, air masses arriving from Siberia (cluster 4 in Fig. 3) and Eurasia (cluster 5 in Fig. 3) exhibit the highest average concentrations of σ_{ap}, with the average values corresponding to 0.14 Mm^{-1} and 0.20 Mm^{-1} respectively. Cluster 3 (Arctic Ocean) is most frequent, arriving approximately 31 % of the time, this is followed by cluster 4 (Siberia) at 29%, cluster 1 (North Atlantic) at 19 %, and clusters 2 and 5 contributing to 11% of the air masses. These average contributions vary throughout the year. The annual frequency of the various clusters was examined (see fig. S11). The NA cluster is most present during the summer months (JJA) (NA, cluster 1 in Fig. S11), coinciding with reduced concentrations in σ_{ap} observed on an annual basis (see Fig. 1 for seasonality). The Siberian cluster increases its contribution during the Arctic Haze season (AHZ, FMAM) and decreases its contribution in SUM. The Eurasian cluster is most frequently present during the transition season and the start of the AHZ season (i.e. DJF).

From Fig S12, we can observe that all clusters, except the Eurasian cluster, display a similar decreasing trend in absolute terms (i.e. approximately -0.003 Mm^{-1}yr^{-1} for clusters 1-4). The Eurasian cluster, i.e. cluster 5, is the only transportation pathway which displays a positive trend in terms of seasonal medians, roughly 0.002 Mm^{-1}yr^{-1}. This is in agreement with the

https://doi.org/10.5194/egusphere-2023-940
Preprint. Discussion started: 12 May 2023

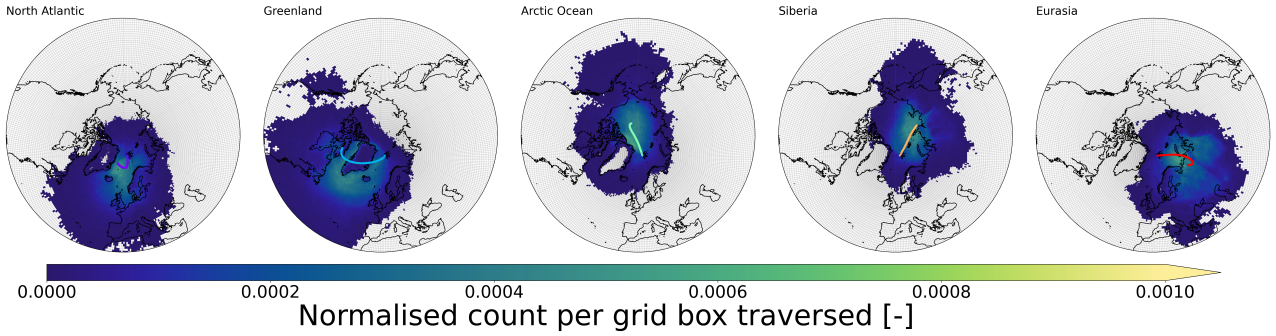

Figure 3. Cluster analysis performed using the latitude, longitude and altitude of all data points in the collocated data set. The length of each back trajectory was set at 10 days. The centroids are shown in each cluster's respective colours, The centroids are arithmetic means of the respective Cartesian coordinates for each endpoint along a back trajectory. The 2-dimensional representation here fails to show the changes in altitude of each respective pathway. The mappings are normalised by dividing by the sum of the entire number of endpoints. The clusters are labelled based on their respective origins (clockwise direction based on the longitude of the last centroid endpoint): cluster 1 corresponds to the North Atlantic (NA) denoted by purple, cluster 2 Greenland (G) denoted by blue, cluster 3 the Arctic Ocean (AO) shown in green, cluster 4 Siberia (S) shown in orange, and cluster 5 Eurasia (E) displayed in red.

CWT trend analysis (see Fig. 2), which shows that southeastern Europe and also central Asia are one of the few regions where there is an increasing trend in terms of their contributions to σ_{ap} measured at ZEP.

3.3.2 Trends in transport pathways:

Based on the clustering (see Fig. 3, in the section above), we can look at the frequency of these clusters over the time span, 2002 - 2022. The occurrence of air masses coming from the North Atlantic region (clusters 1 and 2) has increased since 2002 (see Fig. 4 b). Typically, the NA cluster is one of the cleanest air masses (with a median of $0.049\,\mathrm{Mm}^{-1}$). Figure 4a is based on the same approach used in Hirdman et al. (2010) whereby σ_{ap} is fixed for the various clusters and the trend is predicted based solely on the changes in the frequencies of each respective cluster. Here, the annual mean σ_{ap} shows a decreasing trend. When fixed σ_{ap} values are used (i.e. the fixed values being the average of the first 3 years of each respective cluster: $\sigma_{\mathrm{ap}}^{\bar{\mathrm{NA}}} = 0.24\,\mathrm{Mm}^{-1}$, $\sigma_{\mathrm{ap}}^{\bar{\mathrm{G}}} = 0.24\,\mathrm{Mm}^{-1}$, $\sigma_{\mathrm{ap}}^{\bar{\mathrm{AO}}} = 0.35\,\mathrm{Mm}^{-1}$, $\sigma_{\mathrm{ap}}^{\bar{\mathrm{S}}}, = 0.49\,\mathrm{Mm}^{-1}$, and $\sigma_{\mathrm{ap}}^{\bar{\mathrm{E}}} = 0.47\,\mathrm{Mm}^{-1}$), and then only perturbed based on the respective changes to the frequency of each cluster, no trend is observed (see Fig. 4 a). As a proportion of the trend in the annual mean σ_{ap}, changes in the frequency in the occurrence of each cluster can account for $\approx 2.3\,\%$ of the trend (i.e. -0.0003/-0.013). Note that along with Hirdman et al. (2010), the calculations here are based on the use of arithmetic means, which are more sensitive to outliers, as opposed to medians. The Eurasian air masses (cluster 5) exhibit the largest σ_{ap} values and have increased their contribution from 7% to 15.5%.

https://doi.org/10.5194/egusphere-2023-940
Preprint. Discussion started: 12 May 2023

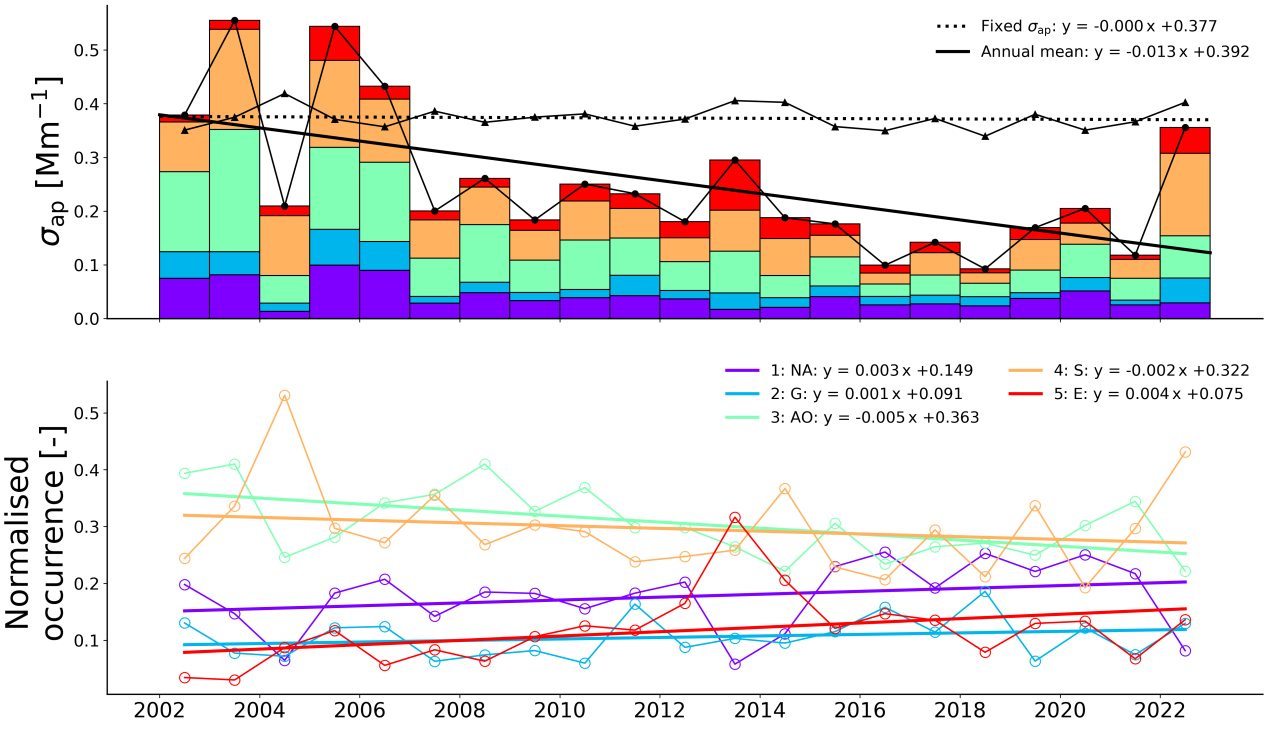

Figure 4. The annual trends in a) the mean absorption coefficient (σ_{ap}) estimated using the least mean square (LMS) and b) the occurrences of each respective cluster, 1-5. Cluster 1 corresponds to the North Atlantic (NA) denoted by purple, cluster 2 Greenland (G) denoted by blue, cluster 3 the Arctic Ocean (AO) shown in green, cluster 4 Siberia (S) shown in orange, and cluster 5 Eurasia (E) displayed in red. In a) each bar representing the annual mean σ_{ap} is subdivided based on the occurrence of each respective cluster. The dashed line describes the trend that would be associated with σ_{ap} if fixed initial values were used and were only perturbed based on the changes in cluster occurrence (frequency).

3.4 Sinks and transport

3.4.1 Trends in precipitation and scavenging ratio

The maximum amount of potential surface precipitation air masses experienced en route to ZEP has increased. The overall trend in mean accumulated back trajectory precipitation (ATP) is approximately $0.15\,\mathrm{mm\,yr^{-1}}$, where the seasonal median ATP increased from 6.3 mm to 9.5 mm, representing a relative annual increase of $2\,\%\mathrm{yr^{-1}}$. The most significant increases in average accumulated precipitation occurred during 2002 - 2012. After 2014, the positive trend in accumulated precipitation appears to stagnate or show a negative trend. The seasonality inherent in ATP is clear from Fig 5. The summer generally (denoted by black triangles in Fig. 5) exhibits the greatest amount of accumulated precipitation, while the Arctic Haze season experiences the least (see S13 b in the supplement).

https://doi.org/10.5194/egusphere-2023-940
Preprint. Discussion started: 12 May 2023

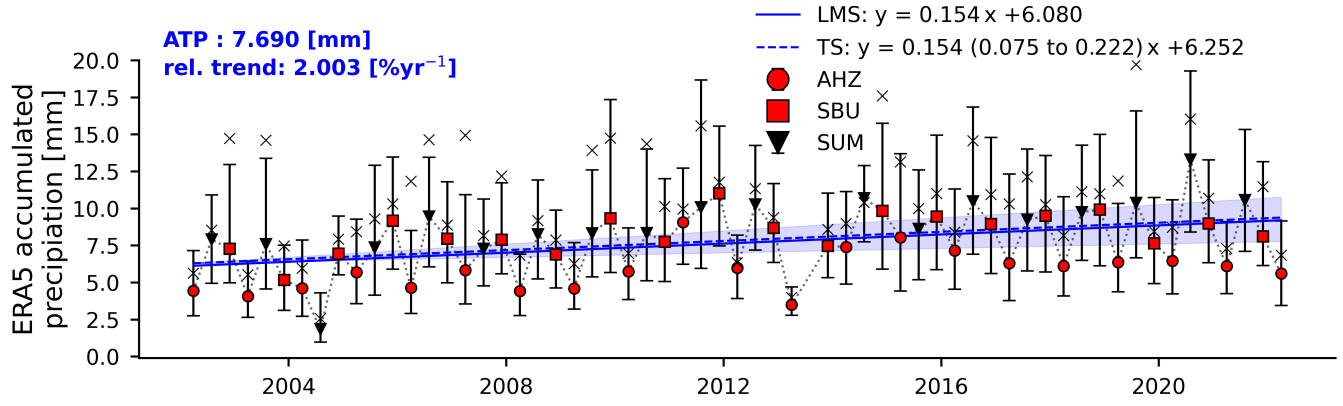

Figure 5. Time series of average accumulated precipitation experienced by 10-day back trajectories arriving at ZEP. The precipitation at the surface is taken from ERA5 reanalysis. The data is not selected such that the air mass is within the mixing layer (ml), instead it is assumed the air mass is influenced by the precipitation regardless of altitude.

The precipitation intensity (i.e. rate) is less for grid cells further north than latitude 79°N. Likewise, back trajectory endpoints experience on average greater rates of precipitation further south. Therefore, special care was taken to show that the trend in average accumulated surface precipitation was present for a given latitude, and thus was not the symptom of back trajectories travelling further south to regions of higher precipitation rates. This is confirmed in the spatial trend analysis of precipitation rates per grid cell (not shown here).

From the analysis of extreme ATP events (see Fig. S14), it was shown that quite some "clean" events, where the σ_{ap} measured at ZEP was extremely low (i.e. within the 1st percentile), coincided with the "wet" events (exceptionally high ATP). Approximately, 14% of the clean days coincided with extreme ATP.

Short-term perturbations in σ_{ap} are in general larger than those of CO suggesting that there is a strong seasonal cycle in aerosol removal processes (see Fig. S15). Aerosol removal processes have a maximum effect (i.e. a minimum value for two scavenging ratios, S_{ap} and S_{sp}) in mid-summer, with the minimum amount of aerosol removal occurring during the Arctic Haze season, as both S_{ap} and S_{sp} exhibit larger values. This seasonality in the scavenging ratio can be seen throughout the period 2002 to 2022 (see Fig. S16). The long-term trend in the scavenging ratio suggests that aerosol removal processes are increasing overall strength (i.e., indicated by a decreasing trend in S_{sp}).

3.4.2 Modelled absorption

In this section, the trend in σ_{ap} is calculated using only accumulated precipitation along the air mass back trajectory (ATP) and the estimated relationships between σ_{ap} and ATP (see Fig. S17). Essentially, here, we explore whether it was possible to reproduce the long-term trend observed in σ_{ap}, using only the increasing trend in ATP and an approximation for the wet removal due to surface precipitation. This acts as an estimate for the contribution in the σ_{ap} trend, deriving from changes in wet removal strength. Roughly, 9 years of data, 2002 - 2010, were utilised to assess the relationship between surface precipitation

https://doi.org/10.5194/egusphere-2023-940
Preprint. Discussion started: 12 May 2023

along back trajectories and in situ observations of σ_{ap}; this relationship was analysed for all three seasons (AHZ, SUM and SBU) and all five source regions (NA, G, AO, S and E) such that 15 empirical relationships are ascertained (see Fig. S17). For the majority of transportation clusters and seasons, there is an exponential decline in σ_{ap} as ATP increases. The extent of the decline varies depending on the cluster and season (see Fig. S17). The summer season experiences the least rate of decline. In general, the clusters that experience the most ATP and the least σ_{ap} values, i.e. North Atlantic 9.2 mm (cluster 1), and Greenland 10.1 mm (cluster 2), exhibit the lowest amounts of wet removal strengths; essentially a large proportion of BC has already been removed from the air masses before they reach ZEP.

The hourly ATP averages are converted to their respective σ_{ap} values using the closest corresponding value for each σ_{ap}-ATP relation (see Fig. S17). To increase the number of data points for each σ_{ap}-ATP relation, a linear interpolation was done between each median value.

The same analysis was performed for monthly values; σ_{ap} (not shown here). The proportion of the trend is approximately the same regardless of the resolution chosen. The seasonality of the predicted σ_{ap} agrees well with the observed σ_{ap}, signifying that ATP is a major factor controlling the annual cycle (see also Section 11 in the supplement). In terms of long-term trends, Fig. 7 shows a decreasing trend in the calculated σ_{ap}, suggesting that ATP plays a role in the decline in σ_{ap}. The resultant trend for the calculated seasonal medians of σ_{ap} is approximately -0.001 $Mm^{-1}yr^{-1}$, roughly 25% of the overall trend observations of σ_{ap} (i.e. -0.004 $Mm^{-1}yr^{-1}$).

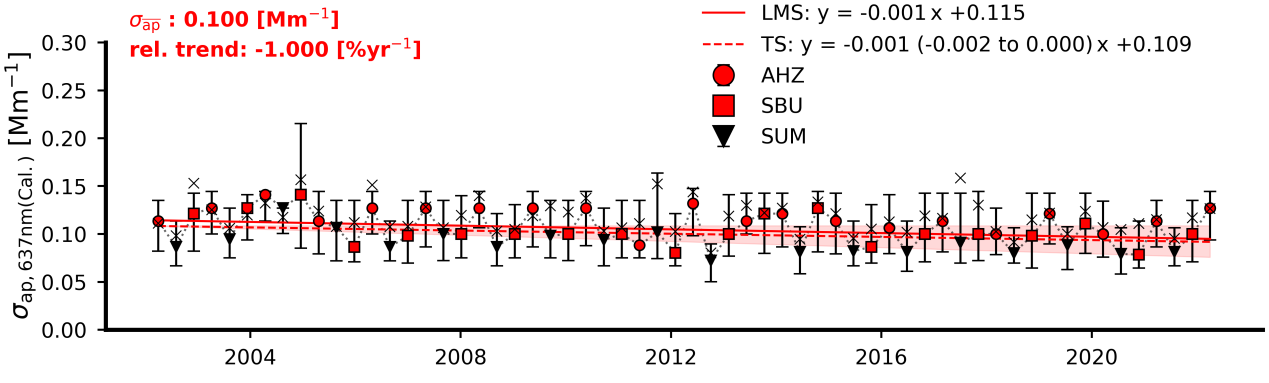

Figure 6. Long-term trend in the calculated absorption coefficient ($\sigma_{ap,637nmcal.}$). The σ_{ap} is estimated using a fixed relationship between σ_{ap} and ATP, and the long-term trends in ATP. Here, the dashed line represented the Theil-Sen Slope, and the solid line represents the LMS line. The seasonal medians are marked in their respective colours and shapes i.e. red circle is the Arctic Haze season (AHZ), red square is the Slow Build-up season (SBU) and the black triangle is the summer season (SUM). The relative trend and overall median value are displayed in the top right-hand corner.

https://doi.org/10.5194/egusphere-2023-940
Preprint. Discussion started: 12 May 2023

3.5 Sources and transport

3.5.1 Biomass burning events

The back trajectories arriving at ZEP have experienced an increasing influence from forest fires. The number of active forest fires each back trajectory traversed over has increased since 2002, with the most notable shift occurring after 2015. The same can be said for the BC emissions, based on the GFED. There are some recent seasons in which the arriving air masses have experienced on average a much higher number of BC emissions. The same can also be seen in the number of active fires; in particular the summer months of 2015, 2016, 2017, 2019 and 2020. Extreme biomass burning events, where the back trajectories traverse grids containing a large number of active fires, exhibit much higher σ_{ap} values (not shown here). However, the number of these events is few and the variability is large. The events are fairly rare due to the requirement of a large number of active fires to be traversed. Overall, from Fig. 7, it is clear that the number of potentially influential biomass-burning events has increased.

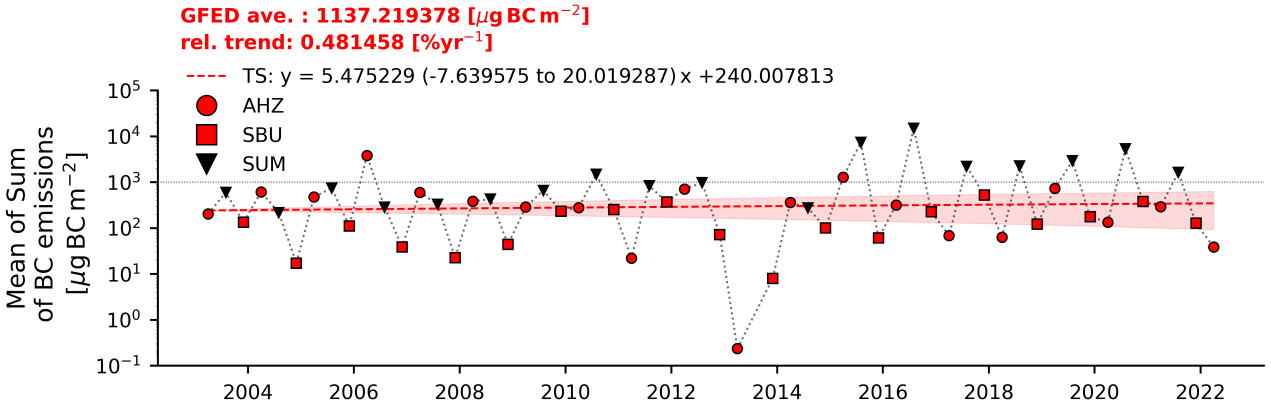

Figure 7. Long-term trend in the average integrated emissions from back trajectories collocated with the Global Fire Emission Data set (GFED). The figure includes the entire data set from 2003 to 2022. Note that the Arctic Haze season (AHZ) of 2006 is significantly smaller compared with the MODIS fire count. The trend is calculated using the Theil-Sen Slope estimator (TS) and the arithmetic seasonal means. Note that the y-axis is displayed on a log scale.

Removing the data points which correspond to the most extreme number of active forest fires (i.e. defined as the 99$^{\mathrm{th}}$ percentile of a running 15-day average), reduces the seasonal means, however, has a negligible effect on the seasonal median. The substantial increase in the number of active fires back trajectories traverse over has no impact on the long-term trend and in particular the trend in the last 7 years.

https://doi.org/10.5194/egusphere-2023-940
Preprint. Discussion started: 12 May 2023

4 Discussion

The Zeppelin Observatory (ZEP) has transitioned from experiencing high seasonal σ_{ap} averages, in particular during the Arctic Haze period, to exhibiting distinctly lower values. The decreasing trend in σ_{ap} is statistically significant (s.s.) and approximately -0.004 or -0.001 $Mm^{-1}yr^{-1}$, depending on the pre-whitening treatment and resolution. All seasons exhibit a s.s. decreasing trend, suggesting that the Arctic Haze is not the only season which experiences an anthropogenic influence. This trend relates to one of the longest time series of light-absorbing aerosol in the Arctic. The most recent period, 2016 - 2022, has witnessed a slight s.s. increasing trend during the Arctic Haze season of 0.001 $Mm^{-1}yr^{-1}$. This shift in sign and the general reduction in the rate of decrease has been referred to as a "stagnation" (Schmale et al., 2022). In addition to σ_{ap}, SSA was shown to have increased from a seasonal average of 0.9 to near unity; thus, we can conclude that the amount of scattering in relation to the absorption has increased at ZEP (see Fig. S3 and S8).

Here, we make the assumption that the observed trends can be explained as the result of either one or more of the following factors: (i) sources: changes in BC emissions, both anthropogenic and natural, (ii) transport: changes in the frequency of various different transportation pathways, and (iii) sinks: alterations in the ability and amount of removal taking place as the aerosol particles are transported to ZEP.

The Eurasian continent has been shown to be one of the most important contributors to BC measured at ZEP (see Fig. S9); a finding which is in agreement with multiple other studies (Hirdman et al., 2010; Backman et al., 2014; Stathopoulos et al., 2021). The fact that this region contributes most to observations of σ_{ap} is the result of a combination of source strength, transportation, and removal processes. During the Arctic Haze season, air masses coming from the direction of Siberia and Eurasia are more frequent (see Fig. S11) and are able to transport pollutants effectively to the Arctic. Furthermore, less precipitation is experienced by air masses during the Arctic Haze season (see Fig. S13 b), meaning that the aerosol particles undergo less removal. An area of particular interest is the Yamal-Nenets gas flaring region in central Russia; this potential source appears in Fig. S9 in 2005, where there are elevated CWT values (AMAP, 2015; Stohl et al., 2013; Klimont et al., 2017; Stathopoulos et al., 2021). It also appears as the region exhibiting the largest reductions in CWT (see Fig. 2). Recent global emission inventories, including ECLIPSE V5a/V6b, have noted that emissions in BC have decreased in regions affecting the Arctic such as Western Europe, the USA and "Russia +" in the period 2000 to 2010, with "Russia +" exhibiting one of the largest relative reductions (Klimont et al., 2017). Previous analysis of long-term trends has suggested that the declines in wintertime BC in the Arctic are the result of emissions changes in the Former Soviet Union (Sharma et al., 2013), despite increasing BC emissions from source regions such as East Asia. In Sharma et al. (2013), modelled BC was overestimated by a factor of three at ZEP. In this work, we have seen that the spatial trends related to the CWT maps display large reductions for the central Russian region, whilst southeast Europe experiences an increased CWT value (see Fig. 2). This finding that air masses originating from the direction of southeast Europe and also east of SE Europe is supported by the trend analysis of the various clusters; the Eurasian cluster (cluster 5 in Fig. S12) experiences a small positive trend in σ_{ap}, equivalent to 0.002 $Mm^{-1}yr^{-1}$. Moreover, the emission inventories related to central Europe, along with Turkey, the Middle-east and parts of central Asia (i.e. "Asia-Stan" as described in Klimont et al., 2017) are purported to have witnessed increased emissions of BC, from 2000 - 2010, according to

https://doi.org/10.5194/egusphere-2023-940
Preprint. Discussion started: 12 May 2023

Klimont et al. (2017). This can also be seen in the trend analysis of the same emission inventories (see Fig. S10). The increase in this region southeast of Europe could also be the result of increases in contributions from sources further south; eBC that is transported from the Indo-Gangetic plane over Central Asia into the high Arctic (Backman et al., 2014).

One such factor, which could explain the increases in source strengths of BC is the emissions from biomass burning (BB) events. Wildfires have led to an increase in BC emissions in the Arctic in recent years (McCarty et al., 2021) and it has been suggested that forest fires are also becoming more frequent and severe (Rogers et al., 2020). This source has been shown to dominate the σ_{ap} measurements during summer (Winiger et al., 2019), however, it remains unknown whether or not this dominance during the summer is a new phenomenon (Schmale et al., 2022). Trying to understand the potential role BB events can have on recent trends in the Arctic was one of the main research questions of this work. We have shown that large BB events are connected to increased σ_{ap} values. Even though there are several examples of high BB episodes observed at Arctic sites, caused by emissions from fires (e.g. Stohl et al., 2007), no increased contribution during the fire season has been shown so far in the trends of σ_{ap}. The reason for the lack of a signature has been explained by the fact that BC from BB events are emitted into the atmosphere further aloft (absence of down-mixing to the boundary layer). In this study, it was shown that the potential influence from BB events has increased (see Figs. 7), and that during particular seasons these events can have a noticeable influence on the σ_{ap} mean. For particular seasons, extreme BB events can comprise a significant proportion of the extreme σ_{ap} events, however, there is a great deal of interannual variability. When the extreme BB events were removed (equivalent to just 3% of the data) from the time series, it was shown that these events can have a significant impact on seasonal mean σ_{ap} values, and therefore these events can alter the long-term trend if calculated based on arithmetic means. Here, though, we report the trends using seasonal medians and as a result, extreme events such as BB events do not possess the ability to alter the magnitude or sign significantly. In future analysis, it may be interesting to examine when the potential influence of a large number of active forest fires does not translate to elevated averages for σ_{ap}; under what conditions do potential emissions of BC not make it to ZEP. It must also be stressed that this increased influence from forest fires only acts as a potential, whether or not the emissions arrive is another question as wet scavenging can play a major role in the removal of aerosol particles before they reach the Arctic. The Arctic is undergoing fundamental changes with increased influence from forest fires. It is expected that the Arctic will be perturbed more and more by BB events.

In regards to changes in transportation, we showed that ZEP has experienced large changes in recent years related to the frequency of various air masses (see Fig. 4 b). Most prominently the North Atlantic and Greenland clusters have increased in their respective contributions; both of these transportation pathways are associated with little anthropogenic influence and therefore contribute to lower values of σ_{ap} at ZEP. There is an increased contribution from the Eurasian cluster, bringing air masses more influenced by anthropogenic sources. The analysis, displayed in Fig. 4, is an extension of the work performed by Hirdman et al. (2010). Using the arithmetic mean, as opposed to the median, the initial values for σ_{ap} were fixed for each cluster, and no trend was associated with the annual mean controlled solely by the changes to the frequencies of each respective cluster and the initial fixed value used. In line with Hirdman et al. (2010), we argue that the changes in the various frequencies of different transportation pathways are not the main factor explaining the reduction in σ_{ap}. One possible reason for this may be the fact that there is a compensating effect taking place, where despite an increased contribution from cleaner air masses

https://doi.org/10.5194/egusphere-2023-940
Preprint. Discussion started: 12 May 2023

(i.e. Greenland and North Atlantic), there is also an increased contribution from air masses from high-emission regions (i.e. Eurasia). In regards to the increased single-scattering albedo measured at ZEP, this could still be the result of an increased contribution of marine air masses, which bring with them sea spray aerosol consisting of an SSA close unity. Previous studies have suggested that this increase in the contribution of more marine air masses is likely the result of changes in air circulation patterns (Heslin-Rees et al., 2020). The phase of the Scandinavian pattern, a large-scale circulation pattern, was shown to affect the variability in transported BC (Stathopoulos et al., 2021); during the cold period, higher concentrations of BC were present when sources were limited to more northern regions, as opposed to when source regions extended further south, and experienced more wet removal.

In terms of changes to potential aerosol removal mechanisms, accumulated back trajectory precipitation (ATP) was explored in detail in this study. It is well documented that the distinct seasonality of aerosol particles in the Arctic is governed by precipitation (Garrett et al., 2011; Tunved et al., 2013). Tunved et al. (2013) demonstrated that wet removal largely controls the aerosol size distributions observed in the Arctic. Furthermore, Tunved et al. (2013) noted that there is an exponential decrease in particle mass with accumulated precipitation; the reduction in mass is most apparent for the first few incremental increases in ATP. In this study, we show that σ_{ap} also reduces exponentially with an increase in ATP suggesting that BC particles are wet scavenged effectively with the initial increases in ATP. The air masses arriving at ZEP have witnessed increased surface precipitation (see Fig. 5). The periods that experienced the largest reductions in seasonal average σ_{ap} coincided with periods experiencing increasing ATP. The stagnation in σ_{ap} also occurs during a period of little change to ATP. Typically, the precipitation intensity, experienced by air masses, increases at lower latitudes. However, it is argued that the trend in accumulated precipitation is not related to air masses experiencing increased intensities further south. In general, the finding that the air masses have experienced an increase in accumulated precipitation is in keeping with claims that the Arctic is getting wetter, as total precipitation increases (Bintanja, 2018; Yu and Zhong, 2021). It should be noted though that some studies could not observe any significant trends in the precipitation rate in the Arctic over a similar period (Breider et al., 2017). The impact of precipitation on the seasonality of BC in the Arctic has led some to suggest that the future Arctic may be cleaner as a result of the influence of wet scavenging on BC (Jiao and Flanner, 2016). In trying to quantify the degree to which trends in ATP influence the long-term reductions in BC, cluster and season-specific relationships for σ_{ap} and ATP were utilised to try and simulate the long-term trend in σ_{ap}. The relation between ATP and the median σ_{ap} was used on a seasonal basis to account for different precipitation regimes. The simple estimation was able to reconstruct the seasonality in BC well, with the distinctive Arctic Haze events towards the end of winter (when ATP is low). However, the estimated σ_{ap} underestimated any large seasonal averages. Overall, the 21 the year-long trend in σ_{ap} was found to be dependent on the amount of ATP. The trend in the modelled σ_{ap} displayed a quarter of the magnitude of the trend in situ σ_{ap} observations. Thus, we argue, here, that high-latitude precipitation has increased, and as a result, eBC is scavenged more en route to the Arctic leading to a cleaner Arctic. In general, more work is required to see how different aerosol types and different types of precipitation can impact the degree of wet scavenging, and hence estimated σ_{ap}. It should be noted that other parameters are important when analysing wet removal processes. The efficiency of wet deposition can depend on the temperature and type of precipitation, not only the amount; for example, wet deposition efficiency is lower in winter as snow is less effective at removing BC than rain (Croft et al., 2009).

https://doi.org/10.5194/egusphere-2023-940
Preprint. Discussion started: 12 May 2023

Another aspect depends on the hydrophilic fraction of BC; as BC ages, it changes from hydrophobic to hydrophilic. If BC ages more slowly as it is transported to the Arctic, it could mean that the hydrophilic fraction will be larger, and thus it may be less effectively scavenged en route to the Arctic. For a more detailed analysis, more parameters that affect wet scavenging, such as temperature (above 0°C), relative humidity, precipitation type and aerosol chemical composition need to be taken into account as it is not only ATP that controls wet scavenging.

Extreme accumulated precipitation events can have a meaningful impact on the overall arithmetic mean σ_{ap}, such that when periods coinciding with high ATP events are removed from the data set, the mean σ_{ap} decreases. Additionally, in terms of trends it has been seen that extreme precipitation events do not dictate the trends (not shown here); all trends in the seasonal medians seemed to be quite robust to extreme increases in ATP.

In regards, to the recent increasing trend during the AHZ season, it is argued here that the recent increase in σ_{ap} is the potential result of a combination of factors, most notably an increase in the contribution from more generally polluted air masses from Siberia (see Fig 4 b), increases in sources from regions south-east of Europe (Klimont et al., 2017), and a decline in the precipitation scavenging sink in the most recent years (see Fig 5).

5 Conclusions

In this study, we have successfully harmonised absorption and scattering coefficient data at ZEP such that it spans from 2002 to 2022. The length of the data set allows for a unique examination of aerosol optical properties in the Arctic from a climatic-relevant time frame and represents one of the longest aerosol optical time series in the Arctic. In this study, we report that ZEP has experienced declines in σ_{ap} in line with previous trend analysis studies which have detailed reductions in σ_{ap} and/or eBC (Collaud Coen et al., 2020; Schmale et al., 2022; Sharma et al., 2013; AMAP, 2015). In addition to the overall decreasing trend, we note that there has been a shift in the sign of the trend. σ_{ap} displayed a wintertime minimum in 2017.

The optical properties were collocated with back trajectories to try to understand which atmospheric parameters were potential factors in influencing averages, seasonality, and overall long-term trends. Our analysis especially looks at the effect of accumulated precipitation and biomass burning events on the characteristics of atmospheric BC aerosol.

We conclude that the observed trends are not the result of changes in the frequencies of certain transportation pathways, due to the compensating nature of the five prevailing transportation pathways, instead, we argue that changes in sources, along with increases in accumulated back trajectory precipitation (ATP) have governed the decline in σ_{ap}. Reduction in sources is often mentioned as the only factor controlling long-term reductions in BC in the Arctic (Stohl et al., 2013). However, wet scavenging is commonly cited as the controlling factor when it comes to the distinct seasonality seen in the Arctic (Garrett et al., 2011; Shen et al., 2017; Tunved et al., 2013) (see also Section 11). If trends in wet scavenging were to increase in a warmer and wetter Arctic climate, then any further increases in ATP will result in a reduced impact on σ_{ap}. Finally, in regards to additional sources of natural BC such as forest fires, these sources have shown that they can significantly alter seasonal means, however, trends remain robust to their increases in frequency.

https://doi.org/10.5194/egusphere-2023-940
Preprint. Discussion started: 12 May 2023

Data availability. The data of this study will be available on the Bolin Centre Database (DOI and link will be added later).

Code and data availability. The code for this study will be made available on GitHub (link will be added later).

Author contributions. DHR, RK and PZ together designed the study. DHR performed data analysis and wrote the manuscript together with RK with input from all PT, JS, PZ, IR, AK, PT, JS. JS set up the custom-built PSAP at ZEP. RC performed trajectory calculations to 2020. KE provided Aethalometer data. All authors read and commented on the manuscript.

Competing interests. PZ and RK are acting as co-editors with ACP. No further competing interests are applicable.

Acknowledgements. We would like to thank research engineers Birgitta Noone, Tabea Henning, and Ondrej Tesar from ACES and the staff from the Norwegian Polar Institute (NPI) for their on-site support. NPI is also acknowledged for substantial long-term support in maintaining the measurements at Zeppelin Observatory. We would also like to thank Kai Rosman for developing the software we used for the instrumentation at Zeppelin.

We thank the Norwegian Institute for Air Research (NILU) for providing the ambient meteorological data and for maintaining the EBAS database.

https://doi.org/10.5194/egusphere-2023-940
Preprint. Discussion started: 12 May 2023

ACTRIS - Sweden and Horizon-Europe EU Project FOCI (Project 101056783).

Framework Programme Project Grant FORCeS agreement n:o 821205; European Research Council (Consolidator Grant INTEGRATE agreement n:o 865799), Knut and Alice Wallenberg Foundation (project grant ACAS, Wallenberg Scholarship AtmoCLOUD agreements n:o 2021.0169 and 2021.0298).

https://doi.org/10.5194/egusphere-2023-940
Preprint. Discussion started: 12 May 2023

References

Acosta Navarro, J. C., Varma, V., Riipinen, I., Seland, Ø., Kirkevåg, A., Struthers, H., Iversen, T., Hansson, H.-C., and Ekman, A. M.: Amplification of Arctic warming by past air pollution reductions in Europe, Nature Geoscience, 9, 277–281, 2016.

AMAP: AMAP assessment 2015: Black Carbon and Ozone as arctic climate forcers, https://www.amap.no/documents/doc/amap-assessment-2015-black-carbon-and-ozone-as-arctic-climate-forcers/1299, 2015.

Anderson, T. L. and Ogren, J. A.: Determining aerosol radiative properties using the TSI 3563 integrating nephelometer, Aerosol Science and Technology, 29, 57–69, 1998.

Asmi, A., Collaud Coen, M., Ogren, J. A., Andrews, E., Sheridan, P., Jefferson, A., Weingartner, E., Baltensperger, U., Bukowiecki, N., Lihavainen, H., Kivekäs, N., Asmi, E., Aalto, P. P., Kulmala, M., Wiedensohler, A., Birmili, W., Hamed, A., O'Dowd, C., G Jennings, S., Weller, R., Flentje, H., Fjaeraa, A. M., Fiebig, M., Myhre, C. L., Hallar, A. G., Swietlicki, E., Kristensson, A., and Laj, P.: Aerosol decadal trends – Part 2: In-situ aerosol particle number concentrations at GAW and ACTRIS stations, Atmospheric Chemistry and Physics, 13, 895–916, https://doi.org/10.5194/acp-13-895-2013, 2013.

Asmi, E., Backman, J., Servomaa, H., Virkkula, A., Gini, M. I., Eleftheriadis, K., Müller, T., Ohata, S., Kondo, Y., and Hyvärinen, A.: Absorption instruments inter-comparison campaign at the Arctic Pallas station, Atmospheric Measurement Techniques, 14, 5397–5413, 2021.

Backman, J., Virkkula, A., Vakkari, V., Beukes, J., Van Zyl, P., Josipovic, M., Piketh, S., Tiitta, P., Chiloane, K., Petäjä, T., et al.: Differences in aerosol absorption Ångström exponents between correction algorithms for a particle soot absorption photometer measured on the South African Highveld, Atmospheric Measurement Techniques, 7, 4285–4298, 2014.

Bintanja, R.: The impact of Arctic warming on increased rainfall, Scientific reports, 8, 1–6, 2018.

Bodhaine, B. A. and Dutton, E. G.: A long-term decrease in Arctic haze at Barrow, Alaska, Geophysical Research Letters, 20, 947–950, 1993.

Bond, T. C., Anderson, T. L., and Campbell, D.: Calibration and intercomparison of filter-based measurements of visible light absorption by aerosols, Aerosol Science & Technology, 30, 582–600, 1999.

Bond, T. C., Doherty, S. J., Fahey, D. W., Forster, P. M., Berntsen, T., DeAngelo, B. J., Flanner, M. G., Ghan, S., Kärcher, B., Koch, D., et al.: Bounding the role of black carbon in the climate system: A scientific assessment, Journal of geophysical research: Atmospheres, 118, 5380–5552, 2013.

Breider, T. J., Mickley, L. J., Jacob, D. J., Ge, C., Wang, J., Payer Sulprizio, M., Croft, B., Ridley, D. A., McConnell, J. R., Sharma, S., et al.: Multidecadal trends in aerosol radiative forcing over the Arctic: Contribution of changes in anthropogenic aerosol to Arctic warming since 1980, Journal of Geophysical Research: Atmospheres, 122, 3573–3594, 2017.

Collaud Coen, M., Andrews, E., Asmi, A., Baltensperger, U., Bukowiecki, N., Day, D., Fiebig, M., Fjæraa, A. M., Flentje, H., Hyvärinen, A., et al.: Aerosol decadal trends-Part 1: In-situ optical measurements at GAW and IMPROVE stations, Atmos. Chem. Phys., 13, 869–894, 2013.

Collaud Coen, M., Andrews, E., Alastuey, A., Arsov, T. P., Backman, J., Brem, B. T., Bukowiecki, N., Couret, C., Eleftheriadis, K., Flentje, H., et al.: Multidecadal trend analysis of in situ aerosol radiative properties around the world, Atmospheric Chemistry and Physics, 20, 8867–8908, 2020.

Croft, B., Lohmann, U., Martin, R. V., Stier, P., Wurzler, S., Feichter, J., Posselt, R., and Ferrachat, S.: Aerosol size-dependent below-cloud scavenging by rain and snow in the ECHAM5-HAM, Atmospheric Chemistry and Physics, 9, 4653–4675, 2009.

https://doi.org/10.5194/egusphere-2023-940
Preprint. Discussion started: 12 May 2023

Dadashazar, H., Alipanah, M., Hilario, M. R. A., Crosbie, E., Kirschler, S., Liu, H., Moore, R. H., Peters, A. J., Scarino, A. J., Shook, M., et al.: Aerosol responses to precipitation along North American air trajectories arriving at Bermuda, Atmospheric chemistry and physics, 21, 16 121–16 141, 2021.

Dalirian, M., Ylisirniö, A., Buchholz, A., Schlesinger, D., Ström, J., Virtanen, A., and Riipinen, I.: Cloud droplet activation of black carbon particles coated with organic compounds of varying solubility, Atmospheric Chemistry and Physics, 18, 12 477–12 489, 2018.

Draxler, R. R. and Hess, G.: An overview of the HYSPLIT_4 modelling system for trajectories, Australian meteorological magazine, 47, 295–308, 1998.

Eleftheriadis, K., Vratolis, S., and Nyeki, S.: Aerosol black carbon in the European Arctic: measurements at Zeppelin station, Ny-Ålesund, Svalbard from 1998–2007, Geophysical Research Letters, 36, 2009.

Freud, E., Krejci, R., Tunved, P., Leaitch, R., Nguyen, Q. T., Massling, A., Skov, H., and Barrie, L.: Pan-Arctic aerosol number size distributions: seasonality and transport patterns, Atmospheric Chemistry and Physics, 17, 8101–8128, 2017.

Garrett, T. J., Brattström, S., Sharma, S., Worthy, D. E., and Novelli, P.: The role of scavenging in the seasonal transport of black carbon and sulfate to the Arctic, Geophysical Research Letters, 38, 2011.

Gebhart, K. A., Schichtel, B. A., and Barna, M. G.: Directional biases in back trajectories caused by model and input data, Journal of the Air & Waste Management Association, 55, 1649–1662, 2005.

Gilbert, R. O.: Statistical methods for environmental pollution monitoring, John Wiley & Sons, 1987.

Hänel, G.: Radiation budget of the boundary layer: Part II, Simultaneous measurement of mean, 1987.

Hansen, J. and Nazarenko, L.: Soot climate forcing via snow and ice albedos, Proceedings of the national academy of sciences, 101, 423–428, 2004.

Hersbach, H., Bell, B., Berrisford, P., Biavati, G., Horányi, A., Muñoz Sabater, J., Nicolas, J., Peubey, C., Radu, R., Rozum, I., Schepers, D., Simmons, A., Soci, C., Dee, D., and Thépaut, J.-N.: ERA5 hourly data on single levels from 1959 to present., https://doi.org/10.24381/cds.adbb2d47, copernicus Climate Change Service (C3S) Climate Data Store (CDS), Accessed on 12-2023, 2018.

Heslin-Rees, D., Burgos, M., Hansson, H.-C., Krejci, R., Ström, J., Tunved, P., and Zieger, P.: From a polar to a marine environment: has the changing Arctic led to a shift in aerosol light scattering properties?, Atmospheric Chemistry and Physics, 20, 13 671–13 686, 2020.

Hirdman, D., Burkhart, J. F., Sodemann, H., Eckhardt, S., Jefferson, A., Quinn, P. K., Sharma, S., Ström, J., and Stohl, A.: Long-term trends of black carbon and sulphate aerosol in the Arctic: changes in atmospheric transport and source region emissions, Atmospheric Chemistry and Physics, 10, 9351–9368, 2010.

Hirsch, R. M., Slack, J. R., and Smith, R. A.: Techniques of trend analysis for monthly water quality data, Water resources research, 18, 107–121, 1982.

Hsu, Y.-K., Holsen, T. M., and Hopke, P. K.: Comparison of hybrid receptor models to locate PCB sources in Chicago, Atmospheric environment, 37, 545–562, 2003.

Jiao, C. and Flanner, M. G.: Changing black carbon transport to the Arctic from present day to the end of 21st century, Journal of Geophysical Research: Atmospheres, 121, 4734–4750, 2016.

Klimont, Z., Kupiainen, K., Heyes, C., Purohit, P., Cofala, J., Rafaj, P., Borken-Kleefeld, J., and Schöpp, W.: Global anthropogenic emissions of particulate matter including black carbon, Atmospheric Chemistry and Physics, 17, 8681–8723, 2017.

Kopp, C., Petzold, A., and Niessner, R.: Investigation of the specific attenuation cross-section of aerosols deposited on fiber filters with a polar photometer to determine black carbon, Journal of aerosol science, 30, 1153–1163, 1999.

https://doi.org/10.5194/egusphere-2023-940
Preprint. Discussion started: 12 May 2023

Krecl, P., Ström, J., and Johansson, C.: Carbon content of atmospheric aerosols in a residential area during the wood combustion season in Sweden, Atmospheric environment, 41, 6974–6985, 2007.

Krecl, P., Johansson, C., and Ström, J.: Spatiotemporal variability of light-absorbing carbon concentration in a residential area impacted by woodsmoke, Journal of the Air & Waste Management Association, 60, 356–368, 2010.

Li, Y., Tong, D., Ngan, F., Cohen, M., Stein, A., Kondragunta, S., Zhang, X., Ichoku, C., Hyer, E., and Kahn, R.: Ensemble PM2. 5 forecasting during the 2018 camp fire event using the HYSPLIT transport and dispersion model, Journal of Geophysical Research: Atmospheres, 125, e2020JD032 768, 2020.

McCarty, J. L., Aalto, J., Paunu, V.-V., Arnold, S. R., Eckhardt, S., Klimont, Z., Fain, J. J., Evangeliou, N., Venäläinen, A., Tchebakova, N. M., et al.: Reviews and syntheses: Arctic fire regimes and emissions in the 21st century, Biogeosciences, 18, 5053–5083, 2021.

Müller, T., Henzing, J., Leeuw, G. d., Wiedensohler, A., Alastuey, A., Angelov, H., Bizjak, M., Collaud Coen, M., Engström, J., Gruening, C., et al.: Characterization and intercomparison of aerosol absorption photometers: result of two intercomparison workshops, Atmospheric Measurement Techniques, 4, 245–268, 2011a.

Müller, T., Laborde, M., Kassell, G., and Wiedensohler, A.: Design and performance of a three-wavelength LED-based total scatter and backscatter integrating nephelometer, Atmospheric Measurement Techniques, 4, 1291–1303, 2011b.

Ogren, J. A., Wendell, J., Andrews, E., and Sheridan, P. J.: Continuous light absorption photometer for long-term studies, Atmospheric Measurement Techniques, 10, 4805–4818, 2017.

Oshima, N., Kondo, Y., Moteki, N., Takegawa, N., Koike, M., Kita, K., Matsui, H., Kajino, M., Nakamura, H., Jung, J., et al.: Wet removal of black carbon in Asian outflow: Aerosol Radiative Forcing in East Asia (A-FORCE) aircraft campaign, Journal of Geophysical Research: Atmospheres, 117, 2012.

Pedregosa, F., Varoquaux, G., Gramfort, A., Michel, V., Thirion, B., Grisel, O., Blondel, M., Prettenhofer, P., Weiss, R., Dubourg, V., Vanderplas, J., Passos, A., Cournapeau, D., Brucher, M., Perrot, M., and Duchesnay, E.: Scikit-learn: Machine Learning in Python, Journal of Machine Learning Research, 12, 2825–2830, 2011.

Petzold, A. and Schönlinner, M.: Multi-angle absorption photometry—a new method for the measurement of aerosol light absorption and atmospheric black carbon, Journal of Aerosol Science, 35, 421–441, 2004.

Petzold, A., Schloesser, H., Sheridan, P. J., Arnott, W. P., Ogren, J. A., and Virkkula, A.: Evaluation of multiangle absorption photometry for measuring aerosol light absorption, Aerosol science and technology, 39, 40–51, 2005.

Platt, S. M., Hov, Ø., Berg, T., Breivik, K., Eckhardt, S., Eleftheriadis, K., Evangeliou, N., Fiebig, M., Fisher, R., Hansen, G., et al.: Atmospheric composition in the European Arctic and 30 years of the Zeppelin Observatory, Ny-Ålesund, Atmospheric Chemistry and Physics, 22, 3321–3369, 2022.

Quinn, P. K., Shaw, G., Andrews, E., Dutton, E., Ruoho-Airola, T., and Gong, S.: Arctic haze: current trends and knowledge gaps, Tellus B: Chemical and Physical Meteorology, 59, 99–114, 2007.

Rantanen, M., Karpechko, A. Y., Lipponen, A., Nordling, K., Hyvärinen, O., Ruosteenoja, K., Vihma, T., and Laaksonen, A.: The Arctic has warmed nearly four times faster than the globe since 1979, Communications Earth & Environment, 3, 1–10, 2022.

Rogers, B. M., Balch, J. K., Goetz, S. J., Lehmann, C. E., and Turetsky, M.: Focus on changing fire regimes: interactions with climate, ecosystems, and society, Environmental Research Letters, 15, 030 201, 2020.

Ruppel, M., Isaksson, E., Ström, J., Beaudon, E., Svensson, J., Pedersen, C., and Korhola, A.: Increase in elemental carbon values between 1970 and 2004 observed in a 300-year ice core from Holtedahlfonna (Svalbard), Atmospheric Chemistry and Physics, 14, 11 447–11 460, 2014.

https://doi.org/10.5194/egusphere-2023-940
Preprint. Discussion started: 12 May 2023

Ruppel, M. M., Soares, J., Gallet, J.-C., Isaksson, E., Martma, T., Svensson, J., Kohler, J., Pedersen, C. A., Manninen, S., Korhola, A., et al.: Do contemporary (1980–2015) emissions determine the elemental carbon deposition trend at Holtedahlfonna glacier, Svalbard?, Atmospheric Chemistry and Physics, 17, 12 779–12 795, 2017.

Sand, M., Berntsen, T. K., von Salzen, K., Flanner, M. G., Langner, J., and Victor, D. G.: Response of Arctic temperature to changes in emissions of short-lived climate forcers, Nature Climate Change, 6, 286–289, 2016.

Schmale, J., Sharma, S., Decesari, S., Pernov, J., Massling, A., Hansson, H.-C., Von Salzen, K., Skov, H., Andrews, E., Quinn, P. K., et al.: Pan-Arctic seasonal cycles and long-term trends of aerosol properties from 10 observatories, Atmospheric Chemistry and Physics, 22, 3067–3096, 2022.

Schmeisser, L., Backman, J., Ogren, J. A., Andrews, E., Asmi, E., Starkweather, S., Uttal, T., Fiebig, M., Sharma, S., Eleftheriadis, K., et al.: Seasonality of aerosol optical properties in the Arctic, Atmospheric Chemistry and Physics, 18, 11 599–11 622, 2018.

Sen, P. K.: Estimates of the regression coefficient based on Kendall's tau, Journal of the American statistical association, 63, 1379–1389, 1968.

Sharma, S., Ishizawa, M., Chan, D., Lavoué, D., Andrews, E., Eleftheriadis, K., and Maksyutov, S.: 16-year simulation of Arctic black carbon: Transport, source contribution, and sensitivity analysis on deposition, Journal of Geophysical Research: Atmospheres, 118, 943–964, 2013.

Shaw, G. E.: Evidence for a central Eurasian source area of Arctic haze in Alaska, Nature, 299, 815–818, 1982.

Shaw, G. E.: The Arctic haze phenomenon, Bulletin of the American Meteorological Society, 76, 2403–2414, 1995.

Shen, Z., Ming, Y., Horowitz, L. W., Ramaswamy, V., and Lin, M.: On the seasonality of Arctic black carbon, Journal of Climate, 30, 4429–4441, 2017.

Shindell, D. and Faluvegi, G.: Climate response to regional radiative forcing during the twentieth century, Nature Geoscience, 2, 294–300, 2009.

Sinha, P., Kondo, Y., Koike, M., Ogren, J., Jefferson, A., Barrett, T., Sheesley, R., Ohata, S., Moteki, N., Coe, H., et al.: Evaluation of ground-based black carbon measurements by filter-based photometers at two Arctic sites, J. Geophys. Res., 122, 3544–3572, 2017a.

Sinha, P., Kondo, Y., Koike, M., Ogren, J., Jefferson, A., Barrett, T., Sheesley, R., Ohata, S., Moteki, N., Coe, H., et al.: Evaluation of ground-based black carbon measurements by filter-based photometers at two Arctic sites, Journal of Geophysical Research: Atmospheres, 122, 3544–3572, 2017b.

Stathopoulos, V., Evangeliou, N., Stohl, A., Vratolis, S., Matsoukas, C., and Eleftheriadis, K.: Large Circulation Patterns Strongly Modulate Long-Term Variability of Arctic Black Carbon Levels and Areas of Origin, Geophysical Research Letters, 48, e2021GL092 876, 2021.

Stein, A. F., Draxler, R. R., Rolph, G. D., Stunder, B. J. B., Cohen, M. D., and Ngan, F.: NOAA's HYSPLIT Atmospheric Transport and Dispersion Modeling System, Bulletin of the American Meteorological Society, 96, 2059 – 2077, https://doi.org/10.1175/BAMS-D-14-00110.1, 2015.

Stohl, A., Berg, T., Burkhart, J., FjÆaa, A., Forster, C., Herber, A., Hov, Ø., Lunder, C., McMillan, W., Oltmans, S., et al.: Arctic smoke–record high air pollution levels in the European Arctic due to agricultural fires in Eastern Europe in spring 2006, Atmospheric Chemistry and Physics, 7, 511–534, 2007.

Stohl, A., Klimont, Z., Eckhardt, S., Kupiainen, K., Shevchenko, V. P., Kopeikin, V. M., and Novigatsky, A. N.: Black carbon in the Arctic: the underestimated role of gas flaring and residential combustion emissions, Atmospheric Chemistry and Physics, 13, 8833–8855, https://doi.org/10.5194/acp-13-8833-2013, 2013.

https://doi.org/10.5194/egusphere-2023-940
Preprint. Discussion started: 12 May 2023

Stone, R. S., Sharma, S., Herber, A., Eleftheriadis, K., and Nelson, D. W.: A characterization of Arctic aerosols on the basis of aerosol optical depth and black carbon measurementsA characterization of Arctic aerosols, Elementa: Science of the Anthropocene, 2, 2014.

Tunved, P., Ström, J., and Krejci, R.: Arctic aerosol life cycle: linking aerosol size distributions observed between 2000 and 2010 with air mass transport and precipitation at Zeppelin station, Ny-Ålesund, Svalbard, Atmospheric Chemistry and Physics, 13, 3643–3660, 2013.

Van Der Werf, G. R., Randerson, J. T., Giglio, L., Van Leeuwen, T. T., Chen, Y., Rogers, B. M., Mu, M., Van Marle, M. J., Morton, D. C., Collatz, G. J., et al.: Global fire emissions estimates during 1997–2016, Earth System Science Data, 9, 697–720, 2017.

Weingartner, E., Nyeki, S., and Baltensperger, U.: Seasonal and diurnal variation of aerosol size distributions (10< D <750 nm) at a high-alpine site (Jungfraujoch 3580 m asl), Journal of Geophysical Research: Atmospheres, 104, 26 809–26 820, https://doi.org/10.1029/1999JD900170, 1999.

Winiger, P., Andersson, A., Yttri, K. E., Tunved, P., and Gustafsson, O.: Isotope-based source apportionment of EC aerosol particles during winter high-pollution events at the Zeppelin Observatory, Svalbard, Environmental Science & Technology, 49, 11 959–11 966, 2015.

Winiger, P., Barrett, T., Sheesley, R., Huang, L., Sharma, S., Barrie, L. A., Yttri, K. E., Evangeliou, N., Eckhardt, S., Stohl, A., et al.: Source apportionment of circum-Arctic atmospheric black carbon from isotopes and modeling, Science advances, 5, eaau8052, 2019.

Yu, L. and Zhong, S.: Trends in Arctic seasonal and extreme precipitation in recent decades, Theoretical and Applied Climatology, 145, 1541–1559, 2021.

Zhongming, Z., Linong, L., Xiaona, Y., Wangqiang, Z., Wei, L., et al.: WMO/GAW aerosol measurement procedures, guidelines and recommendations, World Meteorological Organization, 2016.